

Topical meeting on advances in reactor computation:  
Salt Lake City, Ut, USA  
28-31 March 1983  
CEA-CONF-6710

A SUB-STRUCTURE METHOD FOR MULTIDIMENSIONAL INTEGRAL  
TRANSPORT CALCULATIONS

FR8303079

A. Kavenoky, Z. Stankovski  
Service d'Etudes des Réacteurs et de Mathématiques Appliquées  
Centre d'Etudes Nucléaires de SACLAY  
91191 GIF SUR YVETTE Cedex (FRANCE)

A new method has been developed for fine structure burn-up calculations of very heterogeneous large size media. It is a generalization of the well-known surface-source method, allowing coupling actual two-dimensional heterogeneous assemblies, called sub-structures. The method has been applied to a rectangular medium, divided into sub-structures, containing rectangular and/or cylindrical fuel, moderator and structure elements. The sub-structures are divided into homogeneous zones. A zone-wise flux expansion is used to formulate a direct collision probability problem within it (linear or flat flux expansion in the rectangular zones, flat flux in the others). The coupling of the sub-structures is performed by making extra assumptions on the currents entering and leaving the interfaces. The accuracies and computing times achieved are illustrated by numerical results on two benchmark problems.

## 1. INTRODUCTION

The integral transport computation methods are very efficiently used for cell and assembly calculations but their computing time increases very rapidly with the size of the medium to be treated.

This drawback is mainly signifying for complex geometry two dimensional calculations. The use of higher order expansions is an efficient improving method<sup>1-2</sup> but this method is unable to treat complex geometries like PWR heterogeneous assemblies. It is worth to be mentioned that the integral transport methods are the only routine methods able to treat these complex geometries.

This paper is devoted to the sub-structure method which improves drastically the efficiency of the integral methods. The sub-structure method is a generalization of the well-known surface-source method and this method may be applied to any geometry ; a sub-structure may be a complex twodimensional geometry (i.e. a 3x3 assembly including a burnable poison cell) and the final geometry may account for any mesh of sub-structures.

The presentation will be divided into three parts ; § 2. is devoted to the theoretical basis of the method and § 3. to its practical implementation and to the methods used for the set of linear equations. § 4. provides a brief description of the ARLEQUIN module which is introduced in the APOLLO<sup>3</sup> module of the NEPTUNE<sup>4</sup> system and presents few numerical results.

## 2. THE SUB-STRUCTURE METHOD

The Sub-Structure Method (SSM) appears to be a two scale method : the twodimensional medium is divided into two dimensional elements  $S_i$  and the global calculation is performed by coupling the various sub-structures.

### 2.1 THE FUNDAMENTAL EQUATIONS

Let us consider a medium  $M \in \mathbb{R}^3$  with space dependent sources  $S(r)$  and cross sections ; the medium  $M$  is divided into  $N$  convex sub-media  $S_i$  with :

$$S_i \cap S_j = \delta_{ij} S_i \quad \bigcup_{i=1}^{i=N} S_i = M$$

The surface of  $M$  is denoted by  $\partial M$  where any usual boundary condition may be applied ; the surface of  $S_i$  is denoted by  $\partial S_i$  and an outer normal  $n_i$  is defined at  $r_i \in \partial S_i$ .

The SSM is easily established in multigroup theory, but for simplicity this presentation will be limited to one velocity formalism and isotropic scattering.

Using the linearity and uniqueness properties of the transport equation (Placzek Lemma<sup>5</sup> and corollaries), the total flux inside  $S_i$  is the solution of the transport equation :

$$r \in S_i \quad \Omega \in 4\pi$$

$$\phi(r) = \int_{S_i} \frac{e^{-\Sigma R}}{4\pi R^2} (\Sigma_S(r')\phi(r') + S(r')) dr' - \int_{\partial S_i} ds \int_{2\pi} \frac{e^{-\Sigma R}}{R^2} \phi(r', \Omega') \Omega' \cdot n_i d\Omega' \quad (1)$$

where :

$$R = |r' - r| \quad \Omega = \frac{r - r'}{R}$$

$$\Sigma R = \int_0^R \Sigma_t(r - s\Omega) ds$$

Eq. 1 may be simplified using the obvious operator formula :

$$r \in S_i \quad \phi = H_i \phi + K_i \phi_i^- + T_i \quad (2)$$

Where  $\phi_i^-$  denotes the entering angular flux on  $\partial S_i$ ,  $H_i \phi$  represents the flux due to scattering inside  $S_i$ ,  $T_i$  is due to the sources and  $K_i \phi_i^-$  to the ingoing flux.

The knowledge of  $\phi$  inside  $S_i$  allows the computation of the outgoing flux on  $\partial S_i$  :

$$r \in \partial S_i \quad \Omega \in 2\pi^+$$

$$\phi(r, \Omega) = \frac{1}{4\pi} \int_0^{S_m} ds e^{-\Sigma_s s} \left( \Sigma_s(r-s, \Omega) \phi(r-s, \Omega) + S(r-s, \Omega) \right) + e^{-\Sigma_s S_m} \phi(r-s_m, \Omega, \Omega) \quad (3)$$

Where  $S_m$  is the length of chord issued from  $r$  in the direction  $\Omega$ .

The equivalent simplified formula is :

$$r \in \partial S_i \quad \Omega \in 2\pi^+$$

$$\phi_i^+ = H_i^+ \phi + K_i^+ \phi_i^- + T_i^+ \quad (4)$$

$H_i^+ \phi$  denotes the part of the outgoing flux due to scattering inside  $S_i$ ,  $T_i^+$  the part due to the sources and  $K_i^+ \phi_i^-$  the part due to the uncollided entering neutrons.

In order to solve the initial problem, the continuity of the angular flux across a sub-structure boundary has to be accounted for ; let us define the set  $\partial S$  of points belonging to sub-structure surface  $\partial S_i$  and not to the medium boundary

$$\partial S = \bigcup_{i=1}^{i=N} \partial S_i \cap \partial M$$

At any  $r \in \partial S$  for any given neutron direction  $\Omega$ , the neutron are outgoing the  $i(r, \Omega)$  sub-structure and entering the  $j(r, \Omega)$  sub-structure : the continuity relation is :

$$r \in \partial S$$

$$\phi_j(r, \Omega) = \phi_i(r, \Omega) \quad (5)$$

$$\Omega \in 4\pi$$

The linearity and uniqueness properties of the transport equation allow to prove that Eq. 2-4-5 are equivalent to the original transport equation.

## 2.2 THE RESOLUTION ALGORITHM

Let us assume that the solution of Eq. 2 is known for each  $S_i$  ; it may be written as :

$$r \in S_i \quad \phi = (I - H_i)^{-1} (K_i \phi_i^- + T_i)$$

And the outgoing angular flux is obtained from Eq. 4 :

$$r \in \partial S_i \quad \Omega \in 2\pi^+$$

$$\phi_i^+ = \left( H_i^+ (I - H_i)^{-1} K_i + K_i^+ \right) \phi_i^- + H_i^+ (I - H_i)^{-1} T_i + T_i^+ \quad (6)$$

In Eq. 6, the general reflexion Green's kernel  $R_i$  for  $S_i$  appears ; it accounts for any number of collisions :

$$r \in \partial S_i, \quad \Omega \in 2\pi^+, \quad r' \in \partial S_i, \quad \Omega' \in 2\pi^- :$$

$$R_i(r, \Omega, r', \Omega') = H_i^+(I - H_i)^{-1} K_i + K_i^+$$

As a final result, a simple formula is obtained

$$\begin{aligned} r \in \partial S_i \quad \Omega \in 2\pi^+ \\ \phi_i^+ = R_i \phi_i^- + V_i \end{aligned} \quad (7)$$

Eq. 7 is easily understood as a general reflexion relation for sub-structure  $S_i$  ; in order to solve the original problem Eq. 5 has to be accounted for :

$$\begin{aligned} r \in \partial S \\ \Omega \in 4\pi \\ \phi_j(r, \Omega) = R_i(r, \Omega) \phi_i(r, \Omega) + V_i(r, \Omega) \end{aligned} \quad (8)$$

Eq. 8 is an integral equation dealing only with the angular fluxes on the sub-structure surfaces and the reflexion kernels of the various sub-structures. In this way the initial problem is partitionned into two problems : first obtain the reflexion operator  $R_i$  and second compute the surface sources.

### 3. PRACTICAL IMPLEMENTATION

For a problem to be solved using integral methods, the main benefit of SSM comes from the two step calculation : the collision probabilities are to be calculated for each  $S_i$  with vacuum boundary conditions. This is a huge saving in numerical complexity. However special collision probabilities are to be computed in order to account for the surface sources. The global efficiency of the method depends on the accuracy of the boundary flux representation.

Inside  $S_i$ , integral transport methods are used, the flux is represented as :

$$r \in S_i \quad \phi(r) = \sum_{j=1}^{j=m} \varphi_i^j \pi_i^j(r) \quad (9)$$

If  $S_i$  is divided into  $m$  regions and if  $\pi_i^j$  is the characteristic function of region  $j$ , Eq. 9 is the standard flat flux approximation ; if  $\pi_i^j$  are higher degree polynomials the method is more efficient. These two options are available in our practical implementation.

An unique expansion is used for the angular flux along the sub-structure interface  $\partial S$  ; this unique expansion fulfills evidently Eq. 5.

$$r \in \partial S \quad \Omega \in 4\pi \quad \phi(r, \Omega) = \sum_{\ell=1}^{\ell=P} j^{\ell} \psi^{\ell}(r, \Omega) \quad (10)$$

Restricting this relation to the surface  $\partial S_i$  of  $S_i$  provides :

$$r \in \partial S_i \quad \Omega \in 2\pi^{\pm} \quad \phi_i^{\pm} = \sum_{\ell=1}^{\ell=P} j^{\ell} \Upsilon_i^{\pm}(r, \Omega) \psi^{\ell}(r, \Omega) \quad (11)$$

Where  $\Upsilon_i^{\pm}(r, \Omega)$  are respectively equal to one if  $r$  belongs to  $\partial S_i$  and  $\Omega$  to  $2\pi^+$  (resp.  $2\pi^-$ ) ; those functions are equal to zero in the other case.

Using now a Galerkin technique provides the discretized form of Eqs 2 and 4 :

$$(k = 1 \text{ to } m) \quad \sum_{j=1}^{j=m} a_i^{kj} \varphi_i^j = \sum_{j=1}^{j=m} P_i^{kj} \varphi_i^j + \sum_{\ell=1}^{\ell=P} Q_i^{k\ell} j^{\ell} + T_i^k \quad (12)$$

$$(q = 1 \text{ to } P) \quad \sum_{\ell=1}^{\ell=P} \alpha^{q\ell} j^{\ell} = \sum_{j=1}^{j=n} P_{i+}^{qj} \varphi_i^j + \sum_{\ell=1}^{\ell=P} Q_{i+}^{q\ell} j^{\ell} + T_{i+}^q \quad (13)$$

The set of  $m$  Eq. 12 for each  $S_i$  and  $n$  Eq. 13 allows the calculation of  $m$  values of  $\varphi_i^j$  and  $n$  values of  $j^{\ell}$ .

This treatment is very general ; it allows the use of irregular mesh grids ; the algorithm implemented in the ARLEQUIN accounts for a simpler rectangular geometry which allows a simpler treatment.

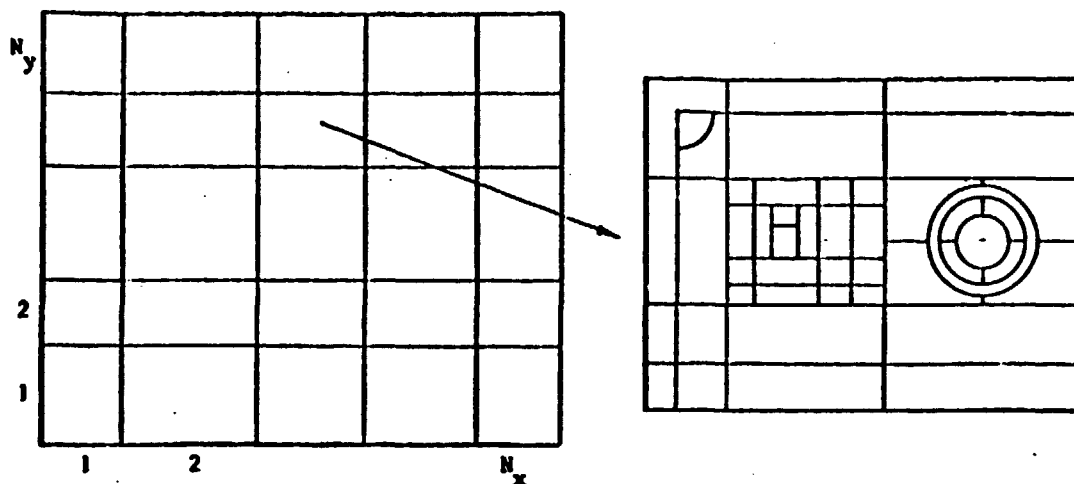
#### 4. THE ARLEQUIN MODULE

The SSM have been implemented in the ARLEQUIN module for rectangular 2D calculations ; the sub-structure collision probabilities are provided by the MARSYAS<sup>2</sup> module and the ARLEQUIN module is introduced in the assembly calculation module APOLLO<sup>3</sup> of the NEPTUNE system for PWR calculations.

ARLEQUIN accounts for any rectangular two-dimensional medium  $M$ .

A rectangular mesh grid divides  $M$  into  $N_x \cdot N_y$  sub-structures ; all the outer boundary conditions useful for practical assembly or reactor calculations are provided. (i.e. vacuum, reflexion translation,  $\pi/2$  or  $\pi$  rotation). Internal black boundary conditions can be simulated by black cells which, of course, are not calculated.

Figure 1. ARLEQUIN Geometry



Each sub-structure  $S_i$  is partitionned into  $m_i$  domains  $d_i^j$  using an eventually irregular mesh grid as shown on Figure 1 ; inside  $S_i$  cylindrical interfaces are accounted for. Internal symetries of any  $S_i$  sub-structures are treated by ARLEQUIN (i.e. half, quarter or diagonal symetries).

#### 4.1 RESULTION ALGORITHM

For the flux representation inside  $S_i$ , two options are available :

- a) Standard flat flux inside  $d_i^j$ ,
- b) linear representation of the flux inside  $d_i^j$  :

$$r \in d_i^j \quad \Phi(r) = a + bx + cy$$

The ingoing flux at the boundary of  $S_i$  is separately represented along each edge of  $S_i$  ; two options are also available :

- a) uniform, isotropic (for  $2\pi^-$ ) ingoing flux along  $\partial S_i^\alpha$ ,
- b) linear,  $P_1$  ingoing flux alont  $\partial S_i^\alpha$ .

The practical representations of internal surface fluxes are :

$$r \in S_i \quad \Phi(r) = \sum_{j=1}^{j=m} \varphi_i^j \pi_i^j(r) \quad (14)$$

$$\begin{aligned} r \in \partial S_i \\ \Omega \in 2\pi^- \end{aligned} \quad \Phi_i^- = \sum_{l=1}^{l=P} j_i^{l-} \omega_i^{j-}(r, \Omega) \quad (15)$$

$$k = 1 \text{ to } m \quad \varphi_i^k = \sum_{j=1}^{j=m} P_i^{kj} \varphi_i^{kj} + \sum_{l=1}^{l=P} Q_i^{kl} j_i^{l-} + T_i^k \quad (16)$$

$$q = 1 \text{ to } q \quad j_i^{q+} = \sum_{j=1}^{j=m} P_{i+}^{qj} \varphi_i^{kj} + \sum_{l=1}^{l=P} Q_{i+}^{kl} j_i^{l-} + T_{i+}^q \quad (17)$$

The set of the  $m$  Eq. 15 is solved for  $q$  values  $\delta_{ql}$  of  $j_i^{l-}$  and the results used in Eq. 17 ; the reflexion matrix is obtained :

$$j_i^{q+} = \sum_{l=1}^{l=P} R_i^{ql} j_i^{l-} + V_i^{q+} \quad (18)$$

Finally Eq. 5 is accounted for and we obtain a set of equations for the ingoing angular fluxes :

$$\sum_{i=1}^{i=n} \sum_{q=1}^{q=P} \alpha_i^{q q'} j_i^{q-} = \sum_{i=1}^{i=n} \sum_{q=1}^{q=P} \beta_i^{q q'} j_i^{q'} \quad (19)$$

This system is solved for  $j_i^{q-}$  and the fluxes inside each  $S_i$  is computed using Eq. 16.

#### 4.2 BENEFITS OF THE SSM

For an integral transport calculation, the most of the computing time is consumed in the collision probabilities calculations. Let us consider a collision probability calculation for a square with  $N \times N$  meshes : the computing time is  $O(N^3)$ . Now let us apply the SSM with  $n \times n$  sub-structures. The number of collision probability calculations is equal to  $n^2$  and each one needs  $O((\frac{N}{n})^3)$ . The time needed by the collision probabilities is reduced by factor  $n$ .

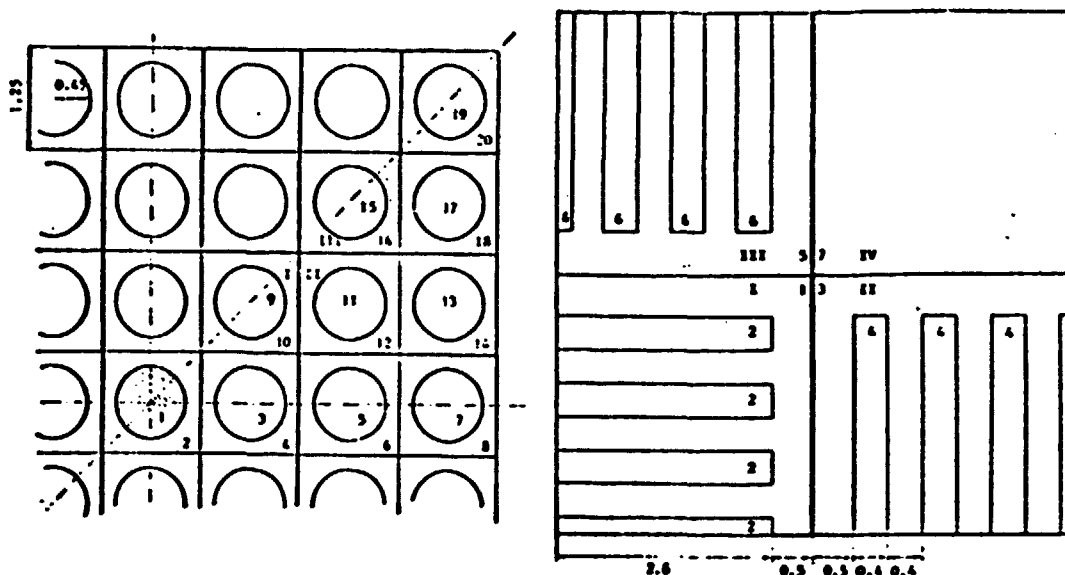
The saving factor may be much larger if internal symetries or boundary conditions are to be accounted for in the initial calculations ; in the usual calculations the long flight of the neutrons across many assemblies are to be followed. If the same sub-structure appears at different locations in the assembly ARLEQUIN performs only one collision probability calculation ; this is an other saving.

The computing time saved during the solution algorithm is also valuable but more difficult to evaluate for it depends on the numerical iteration scheme used.

#### 4.3 NUMERICAL RESULTS

In order to show the accuracy and the benefits of the method two benchmark problems presenting a simplified light wather reactor lattices has been designed for this paper. The geometry and the one-group nuclear data of both problems are shown in Figure 2 and Table 1 ; a spatially constant and isotropically emitting source is present in the moderator.

Figure 2. Geometry of Benchmarks I and II



The Benchmark I consists of a reflected 9x9 pin cell assembly with a central burnable poison rod. The assembly has axial and diagonal symmetry. ARLEQUIN computation uses three sub-structures. Comparison results have been obtained using MARSYAS and NAUSICAA<sup>6</sup>. All calculations have been done in flat flux approximations. Each cell is divided into the moderator and the fuel regions, and each one into four sectors.

Absorption rates in the burnable poison, fuel rods and the moderator are presented on Table 2 ; three results are obtained : a MARSYAS reference result, the ARLEQUIN one and a standard surface-source result obtained by NAUSICAA. The ARLEQUIN maximum error is lower than 1% and the NAUSICAA one may reach 2%.

The assembly of the Benchmark II consists of fuel slabs imbedded in a water moderator ; reflexion boundary conditions are used. The ARLEQUIN results are compared to MARSYAS module ones, in flat flux approximation. In both cases the assembly is divided to 81 regions. The ARLEQUIN computation uses four sub-structures (denoted by roman figures) ; three of them are identical (I, II and III), only one collision probability calculation is performed for these sub-structures.

On Table 3 the ARLEQUIN absorption rates are compared to the standard MARSYAS ones. The accuracy is about 1% and the computing time saving for the entire job is 6 (11 for the collision probability calculations). Computation is performed on a CRAY 1 computer.



## REFERENCES

- 1 Z. Stankovski, "Two Dimensional Treatment of Neutron Transport in a Heterogeneous Medium by Galerkin Method", Thesis of M. of Science, Belgrade 1977.
- 2 A. Kavenoky, M. Lam-Hime, Z. Stankovski, "Improvements of the Integral Transport Theory Method", ANS National Topical Meeting, Computational Methods in Nuclear Engineering, Williamsbure, April 1979.
- 3 A. Kavenoky, "APOLLO : A General Code for Transport, Slowing-down and Thermalization Calculations in Heterogeneous Media", Mathematical Models and Computational Techniques for Analysis of Nuclear Systems, Ann Arbor, Michigan, April 9-11, 1973 (CONF-730414-P1).
- 4 A. Kavenoky, "NEPTUNE : A Modular Scheme for the Calculation of Light Water Reactors", ANS Meeting, Charleston, April 15-17, 1974 (CEA-CONF-3098).
- 5 K.M. Case, F. de Hoffmann, G. Placzek, "Introduction to the Theory of Neutron Diffusion", U.S. Government Printing Office, Washington, D.C. (1953).
- 6 R. Sanchez, "Application de la méthode de Galerkin à la résolution de l'équation intégrale du transport unidimensionnelle", Université de Paris-Sud Thèse de 3ème Cycle, April 1973.

Table 1. Nuclear Data for Benchmark I et II

|                                | <u>Moderator</u> | <u>Fuel</u> | <u>Burnable<br/>Poison</u> |
|--------------------------------|------------------|-------------|----------------------------|
| $\Sigma_t$ (cm <sup>-1</sup> ) | 1.25             | 0.625       | 14.                        |
| $\Sigma_a$ (cm <sup>-1</sup> ) | 0.008            | 0.270       | 14.                        |
| Source<br>Density              | 1.               | 0.          | 0.                         |

Table 2. Comparison of ARLEQUIN results for Benchmark I

| REGION | ABSORPTION RATES |          |              |          |              |
|--------|------------------|----------|--------------|----------|--------------|
|        | MARSYAS          | ARLEQUIN | $\Delta$ (Z) | NAUSICAA | $\Delta$ (Z) |
| 1      | 0.83560          | 0.83820  | 0.31         | 0.82517  | -0.12        |
| 2      | 0.00687          | 0.00688  | 0.01         | 0.00673  | -2.04        |
| 3      | 0.73858          | 0.74040  | 0.25         | 0.73261  | 0.81         |
| 4      | 0.03580          | 0.03580  | 0.00         | 0.03509  | 1.98         |
| 5      | 0.82518          | 0.83188  | 0.81         | 0.82553  | 0.04         |
| 6      | 0.03997          | 0.04014  | 0.42         | 0.03949  | -1.20        |
| 7      | 0.84996          | 0.85424  | 0.50         | 0.85231  | 0.28         |
| 8      | 0.04112          | 0.04122  | 0.24         | 0.04076  | 0.87         |
| 9      | 0.79181          | 0.79168  | -0.02        | 0.79204  | 0.03         |
| 10     | 0.03830          | 0.03814  | -0.42        | 0.03790  | -1.04        |
| 11     | 1.67267          | 1.67210  | -0.03        | 1.67503  | 0.14         |
| 12     | 0.08095          | 0.08052  | -0.53        | 0.08012  | -1.02        |
| 13     | 1.70720          | 1.71032  | 0.18         | 1.71189  | 0.27         |
| 14     | 0.08259          | 0.08236  | -0.28        | 0.08186  | -0.88        |
| 15     | 0.85106          | 0.85517  | 0.48         | 0.85369  | 0.31         |
| 16     | 0.04117          | 0.04118  | 0.02         | 0.04083  | -0.83        |
| 17     | 1.71978          | 1.71779  | -0.12        | 1.72507  | 0.31         |
| 18     | 0.08315          | 0.08273  | -0.50        | 0.08249  | -0.79        |
| 19     | 0.86402          | 0.86263  | -0.16        | 0.86691  | 0.33         |
| 20     | 0.04177          | 0.04155  | -0.53        | 0.04145  | -0.77        |

Table 3. Comparison of ARLEQUIN and MARSYAS Results for Benchmark II

| REGION               | ABSORPTION RATES |          |
|----------------------|------------------|----------|
|                      | MARSYAS          | ARLEQUIN |
| 1                    | 0.4179           | 0.4216   |
| 2                    | 7.1843           | 7.3260   |
| 3                    | 0.5144           | 0.5094   |
| 4                    | 8.7214           | 8.6557   |
| 5                    | 0.5011           | 0.4979   |
| 6                    | 8.7094           | 8.6511   |
| 7                    | 1.4701           | 1.4573   |
| Total                |                  |          |
| Computing Time (sec) | 2.55             | 0.41     |
| $P_{ij}$             |                  |          |
| Computing Time (sec) | 1.400            | 0.128    |

